J Neuropathol Exp Neurol
Vol. 79, No. 4, April 2020, pp. 378–392
doi: 10.1093/jnen/nlz139

ORIGINAL ARTICLE

Fabry Disease With Concomitant Lewy Body Disease

Kelly Del Tredici, MD, PhD, Albert C. Ludolph, MD, Simone Feldengut, Christian Jacob, Heinz Reichmann, MD, Jürgen R. Bohl, MD, and Heiko Braak, MD

Abstract

Although Gaucher disease can be accompanied by Lewy pathology (LP) and extrapyramidal symptoms, it is unknown if LP exists in Fabry disease (FD), another progressive multisystem lysosomal storage disorder. We aimed to elucidate the distribution patterns of FD-related inclusions and LP in the brain of a 58-year-old cognitively unimpaired male FD patient suffering from predominant hypokinesia. Immunohistochemistry (CD77, α-synuclein, collagen IV) and neuropathological staging were performed on 100-µm sections. Tissue from the enteric or peripheral nervous system was unavailable. As controls, a second cognitively unimpaired 50-year-old male FD patient without LP or motor symptoms and 3 age-matched individuals were examined. Inclusion body pathology was semiquantitatively evaluated. Although Lewy neurites/bodies were not present in the 50-year-old individual or in controls, severe neuronal loss in the substantia nigra pars compacta and LP corresponding to neuropathological stage 4 of Parkinson disease was seen in the 58-year-old FD patient. Major cerebrovascular lesions and/or additional pathologies were absent in this individual. We conclude that Lewy body disease with parkinsonism can occur within the context of FD. Further studies determining the frequencies of both inclusion pathologies in large autopsy-controlled FD cohorts could help clarify the implications of both lesions for disease pathogenesis, potential spreading mechanisms, and therapeutic interventions.

Key Words: α-Galactosidase A, α-Synuclein, CD77, Fabry disease, Lewy bodies/neurites, Lysosomal storage diseases, Parkinson disease.

INTRODUCTION

In Gaucher disease (GD), a lysosomal storage disease caused by mutations in the *GBA1* gene leading to a deficiency in the enzyme glucocerebrosidase and accumulations of gylcosylceramide (1), *GBA1* is associated with diverse parkinsonian phenotypes (2–12). Although a substantial literature exists regarding the relationships between GD and Lewy body disease (6, 13–19), less is known about a possible association between Lewy body disease and Fabry disease (FD, or Anderson-Fabry disease) (20–22), which may be more common than GD (23). FD is a relentlessly progressive X-linked recessive multisystem disorder caused by mutations in the *GLA* gene leading to an enzymatic deficiency of α-galactosidase A (α-Gal A) and a continuous accumulation of globotriaosylceramide (Gb3) in vital organs, particularly in the vascular endothelium (23–28).

FD occurs in all ethnicities with an estimated annual incidence of 1:30 000–1:117 000 in males (28, 29), but some sources indicate that FD may be underdiagnosed (23, 30–35). Late-onset forms may occur more frequently than classical early-onset disease (36), and correct diagnosis can be delayed by more than a decade despite symptom onset in childhood (28). The diagnosis is based on confirmation of an FD mutation by genetic analysis of the *GLA* gene, presence of reduced α-Gal A enzyme activity in leucocytes, and elevated plasma Gb3 levels (37, 38). An alternative method is the use of dried blood smears (39). Newborn screening with the goal of optimizing therapeutic interventions to preserve organ function is possible (28, 35). Effective but cost-intensive therapies exist, including enzyme replacement (23, 40–42); however, none of the current options eliminates the need for concomitant adjunctive medications, a personalized therapeutic regimen, and ongoing monitoring (34, 38). Without specific personalized therapy, male patients and a subset of female patients (5, 43) are at risk of developing life-threatening renal, cardiac, or cerebrovascular complications (44).

In addition to parenchymal affection of multiple organs (skin, heart, skeletal muscle, smooth muscle of the gastrointestinal tract, lymph nodes, lung, liver, spleen, pancreas, kidney, adrenal gland, prostate gland), involvement of the peripheral autonomic nervous system (e.g., Auerbach and Meissner plexuses) also has been shown in FD (45–54). The peripheral pathology is accompanied in the central nervous system by progressive accumulation of Gb3-immunoreactive (also designated GL-3, ceramide trihexoside) inclusions in vessel walls and by intraneuronal inclusions in the brain, spinal cord, and dorsal root ganglia (45, 47, 49, 53–58).

From the Clinical Neuroanatomy Section, Department of Neurology, Center for Biomedical Research, University of Ulm (KDT, SF, CJ, HB); Department of Neurology, University of Ulm and DZNE (ACL); Institute for Anatomy and Cell Biology, University of Ulm (CJ), Ulm; Department of Neurology, Dresden University of Technology, Dresden (HR); and Institute of Neuropathology, University of Mainz, Mainz (JRB), Germany.
Send correspondence to: Kelly Del Tredici, MD, PhD, Clinical Neuroanatomy Section, Department of Neurology, Center for Biomedical Research, University of Ulm, Helmholtzstrasse 8/1, 89081 Ulm, Germany; E-mail: kelly.del-tredici@uni-ulm.de
Jürgen R. Bohl and Heiko Braak contributed equally to this work.
This study was supported by Hans & Ilse Breuer Foundation, Frankfurt am Main to HB.
The authors have no duality or conflicts of interest to declare.
Supplementary Data can be found at academic.oup.com/jnen.

Clinical signs in young hemizygous FD males and heterozygous females may be neuropathic pain in the extremities, cutaneous angiokeratosis, hypohidrosis, abdominal colic, dysmotility, diarrhea, nausea, whorled opacities in the corneal epithelium (cornea verticillata), tinnitus (28, 40, 59–62), proteinuria, diabetes insipidus, and, eventually, renal failure. Individuals with adult disease onset can develop hearing loss, vertigo, hypertension, cardiomyopathy, cardiac valvular disease, cardiovascular disease, arrhythmia, cerebrovascular disease, depression, and, sometimes, cognitive decline (25, 30, 63–69). Reports of parkinsonism in FD are infrequent (70–72).

Recently, Nelson et al (73) showed that α-Gal A enzymatic activity was significantly reduced in postmortem brains of 10 individuals with advanced Parkinson disease. However, it is still unknown whether Lewy neurites and Lewy bodies (Lewy pathology, LP) occur in the nervous system of individuals with FD. The only existing report of a coincidence of α-synuclein aggregates and FD is based on an FD experimental mouse model (74). The present study reports the presence of α-synuclein-immunopositive LP in a 58-year-old Fabry patient with neuropathologically confirmed CD77-immunopositive lesions (75).

MATERIALS AND METHODS

Autopsy Cases

This retrospective case study was performed in compliance with university ethics committee guidelines and German state law governing human tissue usage. Informed written consent for autopsy was obtained previously from the patients or their next of kin. Detailed clinical information was ascertained by retrospective review of the patients' medical records, including hospital discharge summaries, and autopsy reports. Study materials included the brain of a cognitively unimpaired 58-year-old white male FD patient, who came to autopsy at the University of Mainz after congestive heart failure with dilated cardiomyopathy of unclear etiology, dyspnea, and progressive renal insufficiency. At the age of 14, he had experienced febrile episodes accompanied by excruciating "rheumatic" joint pains. In adulthood, his doctors had discussed as possible diagnoses for his symptoms a mixed connective tissue disorder and bilateral Raynaud's disease. He had a nearly 30-year history of arrhythmia prior to a third-degree atrioventricular block and cardioverter-defibrillator implantation (76) followed postoperatively by myocardial infarction. He had also suffered 2 small strokes. Clinically, there was no paresis or spasticity. Late in life, one of his doctors noted severe limb hypokinesia, but the patient was not tested at that point for levodopa responsiveness, nor did his medical records indicate whether he had suffered from additional symptoms associated with Lewy body disease, such as hyposmia, autonomic dysfunction, or sleep disturbances (77). FD was initially diagnosed during the general autopsy: Postmortem findings included angiokeratomata in the upper dermal layer of the skin that were especially prominent on the abdomen and around the genitals, severe coronary artery disease, and dilated cardiomyopathy (heart muscle weight: 885 g) (78) accompanied by Gb3 accumulation in cardiomyocytes and endothelial cells of the heart, as well as in the tubular epithelium and endothelial cells of the kidneys. Ultrastructurally, the pathologist found that the accumulations included FD-specific concentric lamellar bodies spaced 5 nm apart (7, 37, 69, 79). These could have been discovered earlier, but the patient had refused an endomyocardial biopsy (69).

Brain tissue embedded in paraffin from a limited number of regions was obtained from a second cognitively unimpaired 50-year-old white male FD patient from the NIH University of Maryland Neurobiobank. This individual came to autopsy following a subarachnoid hemorrhage resulting from a ruptured basilar artery aneurysm (68, 80). No data about α-Gal A levels were available, and it was not reported to what extent he might have received ERT, hematopoietic stem cell transplantation therapy, or therapy with pharmacological chaperones (44, 81). He had undergone kidney transplantation twice because of end-stage renal disease and had recently suffered a stroke with resulting left-sided weakness. He had no history of extrapyramidal signs. Demographic and neuropathological data of both FD patients and 3 neurologically intact individuals used as controls (3 males, age range 50–58 years; mean age 54.3 years) are provided in Table 1.

Genetic Analyses

Apolipoprotein E status was available for four-fifths of the individuals studied (Table 1). The ε4 allele is a major genetic risk factor for sporadic Alzheimer disease (87), TDP-43

TABLE 1. Demographic and Neuropathological Data From the Cases Studied

	F/M	Age	Brain Wt	NFT	Aβ	α-Syn	APOE	Cause of Death
FD								
1	M	58	1320	0	0	4	ε3/4	Congestive heart failure
2	M	50	1450	I	0	0	NA	Ruptured basilar artery aneurysm
Controls								
3	M	50	1315	I	0	0	ε3/3	Malignant neoplasm
4	M	55	1425	I	0	0	ε3/3	Malignant neoplasm
5	M	58	1300	I	0	0	ε2/3	Malignant neoplasm

FD, Fabry disease; F/M, female/male; Age, age in years; Brain Wt, fresh brain weight in grams; NFT, Alzheimer disease-related neurofibrillary stages 0–VI (Gallyas silver-iodide staining) [82, 83]; Aβ, amyloid-β deposition phase 0–5 (Campbell-Switzer pyridine staining, 4G8 immunohistochemistry [83]); α-Syn, Parkinson disease-related neuropathological stages 0–6 (syn-1 immunohistochemistry [84, 85]); APOE, *APOE* allele status [86]; NA, not available.

proteinopathy (88) and, in addition to *GBA1*, for dementia with Lewy bodies (DLB) and Parkinson disease dementia (89–91). *APOE* genotyping was performed using a seminested polymerase chain reaction assay and restriction isotyping with restriction enzyme *Hha*I, as elsewhere (86). Genomic DNA was extracted from formaldehyde-fixed and paraffin-embedded brain specimens using the manufacturer's protocols (QIAamp DNA Mini Kit, Qiagen, Hilden, Germany). The *GLA* variants of both FD patients were not determined at the time of autopsy. Later, repeated attempts to isolate genomic DNA for sequencing in Ulm from the available formaldehyde-fixed brain tissue were unsuccessful because either too little tissue was available (patient 2) and/or the resulting DNA was too fragmentary (patients 1 and 2).

Tissue Embedding, Sectioning, and Staining

The brains of the 58-year-old patient and 3 controls were fixed by immersion in a 4% buffered aqueous solution of formaldehyde for 14 days. The hemispheres were cut perpendicular to Forel's axis into 1-cm-thick slices, and 12 tissue blocks from the right hemisphere together with the entire brainstem were embedded in polyethylene glycol (PEG 1000, Roth, Karlsruhe, Germany) for serial sectioning at 100 µm on a tetrander (Jung, Heidelberg, Germany), as described previously (82, 92). Additional unstained serial tissue sections and brain tissue were stored for subsequent use in a 4% aqueous solution of formaldehyde at 8–15°C. Paraffin blocks from the 50-year-old FD patient were sectioned at a thickness of 100 µm, as elsewhere (93).

Free-floating sections from each case were pretreated with performic acid and stained with aldehyde fuchsine (12763.00500, Morphisto, Frankfurt am Main, Germany) for selective staining of lipofuscin deposits combined with a basophilic Nissl stain (Darrow red, 211885, Sigma-Aldrich, Steinheim, Germany) for topographical overview and to mark neuronal loss (82, 94). Additional sets of free-floating sections were stained with silver methods to visualize neurofibrillary lesions (Gallyas silver-iodide method) and amyloid-β (Aβ) deposition (Campbell-Switzer pyridine method) associated with Alzheimer disease, as recommended previously (82, 83).

Immunohistochemistry

Separate sets of 100-µm free-floating sections from both FD cases were immunostained using the following antibodies: (1) a monoclonal mouse antibody anti-CD77 (1:200; Clone 5B5; BioLegend, San Diego, CA) for recognition of FD-associated Gb3 deposits (75); (2) a monoclonal mouse antibody PHF-Tau (1:2000; Clone AT8; Pierce Biotechnology [Thermo Scientific], Waltham, MA) not only for detection of hyperphosphorylated tau protein in Alzheimer disease and argyrophilic grain disease (83) but also for exclusion of frontotemporal dementia-related tauopathies (95); (3) a monoclonal mouse antibody anti-beta-amyloid (1:5000; Clone 4G8; BioLegend) as a marker of Aβ deposition (83); (4) a monoclonal mouse antibody anti-syn-1 (1:2000; Clone number 42; BD Biosciences, Eysins, Switzerland) for detection of Lewy body disease-related α-synuclein inclusions (83); (5) a polyclonal rabbit antibody anti-collagen IV (1:5000; ab6586, Abcam, Cambridge, UK) for staining vessel wall components (96). Selected pigment-Nissl stained 100-µm sections from each case underwent immunostaining with (6) a polyclonal rabbit antibody TDP-43 recognizing the N-terminal of normal and abnormal TDP-43 (1:5000; Proteintech, Manchester, UK) (97). Additional selected sections containing the Ammon's horn (CA) were immunostained with (7) the monoclonal antibody SMI-311 (1:1000; Covance, Princeton, NJ) for recognition of nonphosphorylated neurofilaments in Cajal-Retzius projection cells (98). Finally, double immunostaining (CD77 plus α-synuclein) was performed on free-floating 100-µm sections from the 58-year-old FD case.

Tissue sections for immunohistochemistry were treated for 30 minutes in a mixture of 10% methanol plus 10% concentrated (30%) H_2O_2 and 80% Tris. Following pretreatment with 100% formic acid for 3 minutes (4G8, syn-1) or microwave for 30 minutes (CD77, SMI-311) or for 60 minutes in citrate puffer (TDP-43) to facilitate the immunoreactions, blocking with bovine serum albumin was performed to inhibit endogenous peroxidase and to prevent nonspecific binding. Subsequently, each set of free-floating sections was incubated for 18 hours at 20°C using the primary antibodies. After processing with a corresponding secondary biotinylated antibody (anti-mouse or anti-rabbit IgG, 1:200; Linaris, Vector Laboratories, Burlingame, CA) for 1.5 hours, all immunoreactions were visualized with the avidin-biotin complex (ABC, Vectastain, Vector Laboratories) for 2 hours and the chromogen 3,30-diaminobenzidine tetrahydrochloride (DAB; D5637, Sigma, St. Louis, MO). In sections double-immunostained for CD77 and syn-1, the CD77 immunoreaction was visualized using the brown chromogen DAB and syn-1 with the dark blue chromogen SK-4700 (SG Substrate Kit, Vector). Omission of the primary antiserum resulted in nonstaining. Positive and negative control sections were included for all immunoreactions. Then, tissue sections were cleared, mounted, and cover-slipped (Histomount, National Diagnostics, Atlanta, GA).

Histological slides were viewed and neuropathological staging performed with an Olympus BX61 microscope (Olympus Optical, Tokyo, Japan). Digital micrographs were taken with an Olympus XC50 camera using the Cell D Imaging Software (Olympus, Münster, Germany). Pathology was assessed semiquantitatively on a 4-point scale: − = none or no detectable inclusions, + = slight (at least 1 or 2 inclusions); ++ = moderate; +++ = severe, and heat maps were created for the semiquantitative data (Tables 1–4; Supplementary Data Tables).

RESULTS

Of the 3 age-matched control individuals, none showed the presence of CD77-positive inclusions or LP; in addition, none displayed TDP-43 proteinopathies (Table 1). Inclusion body pathologies compatible with FTD-related tauopathies, for example, progressive supranuclear palsy, were not present in either of the FD brains or controls. Mild hippocampal sclerosis was noted in the Ammon's horn sector CA1 of the 50-year-old FD patient. In FD, we observed CD77-immunoreactive intraneuronal and astrocytic inclusions as

well as CD77-positive accumulations in the vasculature of both individuals (Tables 2, 3).

CD77-Immunopositive Intraneuronal Inclusions

Lipofuscin deposits were not CD77-immunoreactive (53). Gb3-inclusions were confined to somata, which frequently had a swollen or ballooned aspect (50), and were not seen in dendritic, axonal, or intranuclear compartments. Although Gb3 accumulations were absent in the anterior olfactory nucleus, mitral cell layer, and olfactory tract (Table 2), an additional primary olfactory region, the prepiriform cortex, displayed pronounced CD77-positive intraneuronal involvement (Table 2; Fig. 1A). In the lower medulla, Gb3 storage was most abundant in the large preganglionic neurons of the dorsal motor nucleus of the vagal nerve (X) and in nerve cells of the surrounding glossopharyngeus-vagus nuclear complex (including the inferior salivatory nucleus and area postrema) (Table 2; Fig. 1B), in the prepositus nucleus of the hypoglossal nerve, the motor nucleus of the facial nerve (VII) in the lower pontine tegmentum and in the motor nucleus of the trigeminal nerve (V), as well as in the dorsal raphe (supratrochlear) nucleus (Table 2; Fig. 1C, D). Extraneuronal remnants of Gb3 deposits marked nerve cell loss, for example, in the motor nucleus of the facial nerve (Fig. 1E). The oculomotor (III) and abducens (VI) nuclei were unremarkable. The neuromelanin-containing nerve cells in the glossopharyngeus-vagus nuclear complex and adjoining intermediate reticular zone (A1/A2 catecholaminergic groups) (99) were spared, as were the gracile and cuneate nuclei of the dorsal medulla and the neuromelanin-containing neurons of the locus coeruleus (A6 group).

Less Gb3 storage was found in the motor nucleus of the hypoglossal nerve (XII), the ambiguus nucleus, in noncatecholaminergic neurons of the intermediate reticular zone, and in nerve cells of the inferior olivary complex (Table 2; Supplementary Data Fig. S1A), as well as in nerve cells at the medial fringe of the vestibular nuclei, in the great raphe nucleus, gigantocellular nuclei of the reticular formation (Table 2), trochlear nucleus (IV) (Table 2), midbrain pedunculopontine nucleus, and in noncatecholaminergic nerve cells of the pars compacta and pars reticulata of the substantia nigra (Table 2). The pigmented parabrachial nucleus (A10 group) and noncatecholaminergic neurons of the paranigral nucleus displayed more storage activity than the nigral pars compacta and pars reticulata (Table 2), whereas neuromelanin-containing neurons of the paranigral nucleus (A10 group) and nerve cells in the red nucleus were unremarkable (99). Also unremarkable were the neurons of the arcuate nucleus together with those in other precerebellar nuclei. Gudden's (dorsal tegmental) nucleus contained no Gb3 accumulations.

Among other involved subcortical nuclei, the central (Supplementary Data Fig. S1E), basal, and accessory cortical (olfactory) subnuclei of the amygdala displayed a heavy burden of CD77-immunoreactive neurons (Table 2; Fig. 1F). As reported earlier, abundant Gb3 storage occurred in the hypothalamus (supraoptic and paraventricular nuclei) (49–51, 53; but compare 100) (Table 2). The hypothalamic tuberomamillary nucleus and thalamus were devoid of intraneuronal inclusions (53). Isolated Gb3 accumulations were present in nerve

TABLE 2. Regional Distribution and Severity of Fabry Disease Intraneuronal CD77-Positive Gb3 Inclusions in 2 Cases

Case		1	2
olf	Olfactory bulb/tract	−	−
dm	Dorsal motor nucleus of the glossopharyngeal and vagal nerves (IX/X)	+++	++
am	Ambiguus nucleus	+	+
irz	Intermediate reticular zone	++	+
io	Inferior olivary complex	+	++
hn	Motor nucleus of the hypoglossal nerve (XII)	+	+
rm	Great raphe nucleus	+	NA
gig	Gigantocellular nucleus of the reticular formation	+	NA
ph	Prepositus hypoglossal nucleus	+++	NA
su	Subventricular nucleus	+	NA
fa	Motor nucleus of the facial nerve (VII)	+++	NA
pc	Central reticular nucleus of the pons	++	NA
tri	Motor nucleus of the trigeminal nerve (V)	+++	NA
dr	Dorsal raphe (supratrochlear) nucleus	+++	−
sn	Substantia nigra, pars compacta & pars reticulata	+	−
pa	Paranigral nucleus	+	NA
pg	Pigmented parabrachial nucleus	++	NA
ppt	Pedunculopontine tegmental nucleus	+	NA
tro	Trochlear nucleus (IV)	+	NA
ce	Central nucleus of the amygdala	+++	NA
ba	Basal nucleus of the amygdala	+++	++
la	Lateral nucleus of the amygdala	+	−
ct	Cortical nucleus of the amygdala	++	NA
ac	Accessory cortical nucleus of the amygdala	+++	+++
db	Interstitial nucleus of the diagonal band	+	+
bn	Basal nucleus of Meynert	+	NA
ts	Bed nucleus of the terminal stria	++	NA
so	Hypothalamic supraoptic nucleus	+++	+++
pv	Hypothalamic paraventricular nucleus	+++	NA
CA4	Ammon's horn, fourth sector	(+)	−
pro	Prosubiculum	+++	+++
tre	Transentorhinal region layer pri-β	+++	NA
ent	Entorhinal region layer pri-β	+++	+
pi	Prepiriform cortex (Brodmann Area 51)	+++	NA
mol	Cajal-Retzius cells in the molecular layer between the dentate fascia and Ammon's horn on both sides of the hippocampal fissure	+++	NA
fu	Fusiform gyrus, layers I and Vb	+++	NA
it	Inferior temporal gyrus, layer Vb	+++	NA
mt	Medial temporal gyrus, layer Vb	+	NA
st	Superior temporal gyrus, layer Vb	+	+
in	Insula	+++	NA
ai	Agranular insular cortex, layer I Cajal-Retzius cells	++	NA
ci	Anterior cingulate gyrus, layer I Cajal-Retzius cells	++	NA
pm	Primary motor area Betz cells (Brodmann Area 4)	(+)	NA
vis	Primary visual cortex, layer I Cajal-Retzius cells (Brodmann Area 17)	+	NA
vh	Spinal cord ventral horn α-motoneurons (layer 9)	+	NA
IML	Intermediolateral nucleus (layer 7)	++	NA

The pathology was assessed semiquantitatively: −, absent or not detectable; +, slight; ++, moderate; +++, severe. Only regions with CD77-positivity are shown. For accompanying heat map, see Supplementary Data Table.
NA, not available.

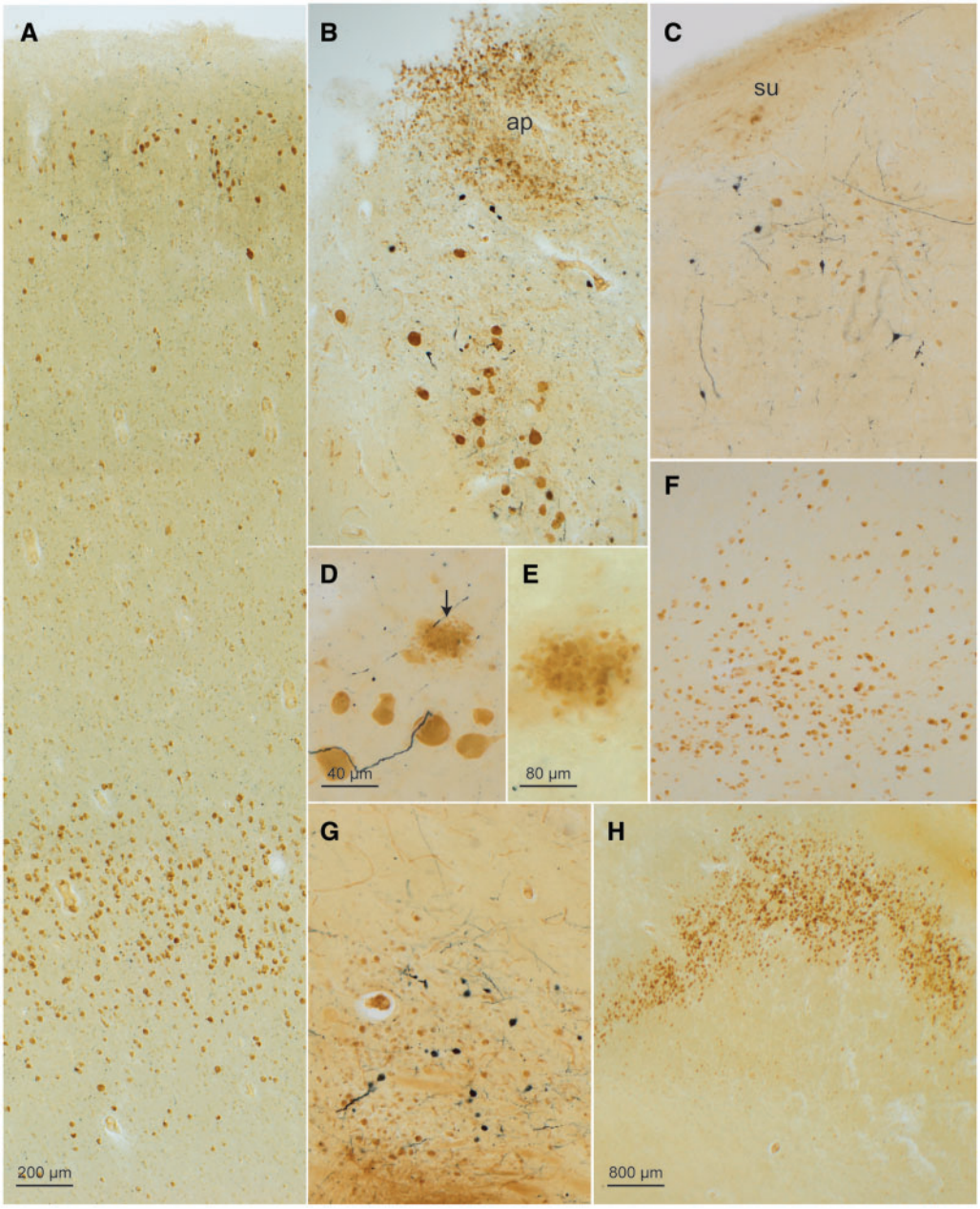

FIGURE 1. CD77-immunopositive intraneuronal inclusions in a 58-year-old male with Fabry disease. **(A)** Gb3 accumulations (DAB, brown chromogen) occurred chiefly in nerve cells of the superficial cellular layers (II and IIIa) and deep layer (V) of the prepiriform cortex (Brodmann Area 51). The afferents to this area originate in the olfactory bulb, retrobulbar region, olfactory tubercle, septal region, amygdala, orbitofrontal cortex, and contralateral piriform cortex. The connectivity of the piriform cortex indicates its role as a link between the olfactory and limbic system. Also detectable in this micrograph, upon closer inspection, in the upper and lower cellular layers is syn-1-immunopositive Lewy pathology (SK-4700, dark blue chromogen). **(B)** Gb3 inclusions in nerve cells of the dorsal motor nucleus of the vagal nerve and in astrocytes of the area postrema (ap) of the glossopharygeus-vagus nuclear complex. In addition, Lewy pathology (LP) was present in the somata and cellular processes of nerve cells in the dorsal motor nucleus of the vagal nerve (SK-4700). **(C)** The prepositus hypoglossal nucleus also displayed Gb3 inclusions (DAB) and LP (SK-4700). A few nerve cells in the subventricular nucleus (su) were also CD77-positive. **(D)** Gb3 accumulation in motoneurons (DAB) of the motor nucleus of the facial nucleus accompanied by Lewy neurites (dark blue chromogen) and extraneuronal remnants of Gb3 (arrow) marking cell loss **(E)** there. **(F)** CD77 immunoreactivity (DAB) in nerve cells of the cortical accessory nucleus of the amgydala. **(G)** Gb3 inclusions (DAB) in nerve cells of the cholinergic nucleus of the diagonal band (similar pathology was also present in the basal nucleus of Meynert and bed nucleus of the terminal stria of the same case). **(H)** Severe intraneuronal Gb3 pathology in the prosubiculum. Immunonegative portions below the wave-shaped prosubiculum belong to pyramidal layers of the subiculum. Immunoreactions: CD77 (DAB, brown chromogen) or CD77 (DAB) plus syn-1 (SK-4700, dark blue chromogen) in 100 µm sections. Scale bar in **(A)** applies to **(B)**, **(C)**, **(F)**, and **(G)**.

cells of two cholinergic nuclei of the basal forebrain: the basal nucleus of Meynert and bed nucleus of the diagonal band (Table 2; Fig. 1G). The nerve cells of the caudate nucleus, putamen, pallidum, and claustrum contained no Gb3 deposits.

In the Ammon's horn of the hippocampal formation, a single CD77-positive nerve cell was present in sector CA4. Otherwise, sectors CA3–4 were devoid of intraneuronal pathology (Table 2). By contrast, very abundant Gb3 accumulations occurred in superficial pyramidal cells of the prosubiculum in CA1 (Table 2; Fig. 1H) as well as in SMI-311-immunopositive Cajal-Retzius cells of the molecular layer located between the dentate fascia and sector CA1, close to the hippocampal fissure (Table 2; Fig. 2C). Notably, CD77-positive Cajal-Retzius cells were also found in layer I of the agranular insular cortex, anterior cingulate gyrus, and neocortical fields, including the primary visual neocortex (Table 2; Fig. 2A, B).

The pri-β layers of the transentorhinal and entorhinal cortex displayed abundant CD77-immunopositive nerve cells (Table 2). In both regions, only a few neurons in layers pre-α and pre-β contained Gb3 deposits, whereas the remaining cellular layers (pre-γ, pri-α, pri-γ) were completely spared.

Pyramidal cells with intraneuronal Gb3 accumulations filled layer Vb of the occipitotemporal fusiform (Fig. 2D) as well as inferior temporal gyri. Fewer deposits were found in the medial temporal and superior temporal gyri, with a complete sparing of the transverse gyrus of Heschl (Table 2). The pyramidal cells of the insula contained abundant Gb3 inclusions. Layer Vb pyramidal cells in the anterior cingulate gyrus displayed moderate involvement; the von Economo neurons there were unremarkable (101). A single Betz pyramidal cell in layer Vb of the primary motor neocortex was CD77-immunopositive (Table 2). No Gb3 storage occurred in the Meynert cells in layer Vb of the primary visual neocortex.

As reported elsewhere for the cerebellum in FD (53), nearly the entire row of Purkinje cells situated at the border of the granular and the molecular layers was obliterated, such that very few Gb3 deposits there were CD77-positive. Nerve cells containing Gb3 accumulations were not observed in the cerebellar dentate nucleus or cerebellar cortex (53). In sections from the thoracic spinal cord, several α-motoneurons in layer 9 of the ventral horn stored Gb3 and the viscerosensory neurons of the intermediolateral nucleus in layer 7 were moderately involved (Table 2). The dorsal root was not available for evaluation (49–51, 53, 57).

CD77-Immunopositive Astrocytic and Vascular Inclusions

Numerous astrocytes with Gb3 accumulations surrounded the glomerula of the olfactory bulb and filled cells of the granule layer as well as the olfactory tract (Table 3; Fig. 3A, B). Apart from these sites, the remaining CD77-positive astrocytic pathology was consistently seen in regions close to blood vessels and in regions with direct contact to cerebrospinal fluid (ventricular subependyma) (50), choroid plexus epithelium separating the blood and the ventricular cerebrospinal fluid, portions of the fornix (Fig. 2E), and subarachnoidal spaces (Supplementary Data Fig. S1C). Remarkable thereby was the decreasing gradient in CD77 staining intensity the greater the distance from the ventricle (Supplementary Data Fig. S1C). The meninges were less severely affected than the subependymal zone. Both the somata and perivascular end-feet of astrocytes accumulated Gb3. Other types of glia cells (oligodendrocytes, microglia) did not store CD77.

Severe astrocytic Gb3 accumulations were abundant in the area postrema and gelatinosus nucleus of the glossopharyngeus-vagus nuclear complex (Table 3; Fig. 1B) as well as in the ependyma and subependyma there but also in the hypothalamus (Fig. 2E). Elsewhere in the medulla, CD77-positive astrocytes formed a band along the ribbon of small cells and vessels of the inferior olivary complex (Table 3). Subependymal astrocytes (somata, perivascular end-feet close to the ventricle and especially to the foramen of Lushka) were CD77-positive. In CA1, at the transition to lateral ventricle, astrocytic involvement of the subependymal stratum album (alveus) was remarkably severe. Moderate astrocytic CD77-storage occurred in the pallisades of Bergmann glia extending into the molecular layer of the cerebellum and along blood vessels of the dentate nucleus and in the cerebellar stratum granulosum (Table 3).

In both FD brains, Gb3 deposits in the endothelium of large and small blood vessels were widespread (Fig. 2F) that were not present in controls. In FD, vessels showing Gb3 accumulations were also frequently tortuous (49, 102, 103) (Fig. 2G; Supplementary Data Fig. S1B). Evidence of 2 small cerebrovascular insults (subiculum, occipital lobe) was found in the older FD patient (Fig. 2G).

α-Synuclein-Immunopositive Lewy Neurites and Lewy Bodies

In the older FD patient, LP was observed in regions and neuronal types known to become involved in Parkinson disease and DLB (84, 104, 105). This pathology included somatic, axonal, and somatodendritic inclusions. Immunoreactive oligodendrocytes were not present. Severe lesions were present in the olfactory bulb, mitral cells, anterior olfactory nucleus, and olfactory tract (Table 4; Fig. 3A, B), as well as in the locus coeruleus (with neuronal loss in the A6 group), dorsal raphe nucleus (Supplementary Data Fig. S1D), substantia nigra (with severe neuronal loss in the pars compacta, A9 group), and tegmental pedunculopontine nucleus (85) (Table 4; Fig. 3C–E).

LP was also present within the large visceromotor neurons of the dorsal motor nucleus of the vagal nerve (Table 4; Figs. 1B and 4D), in nerve cells of the medullary intermediate reticular zone, where the intramedullary axons of the vagal nerve were also strongly α-synuclein-immunopositive (84) (Fig. 3F), and in neurons of the great raphe nucleus and of the gigantocellular nuclei in the reticular formation (Table 4; Fig. 4A), prepositus hypoglossal nucleus (Fig. 1C), motor nucleus of the facial nerve (Fig. 1D), amygdalar accessory cortical and central nuclei (Table 4; Fig. 4B), basal forebrain nucleus of Meynert and bed nucleus of the diagonal band (Table 4; Fig. 1G), and the hypothalamic tuberomamillary nucleus (84) (Table 4; Fig. 4C). In the external capsule, axons projecting from the cholinergic nuclei of the basal forebrain to

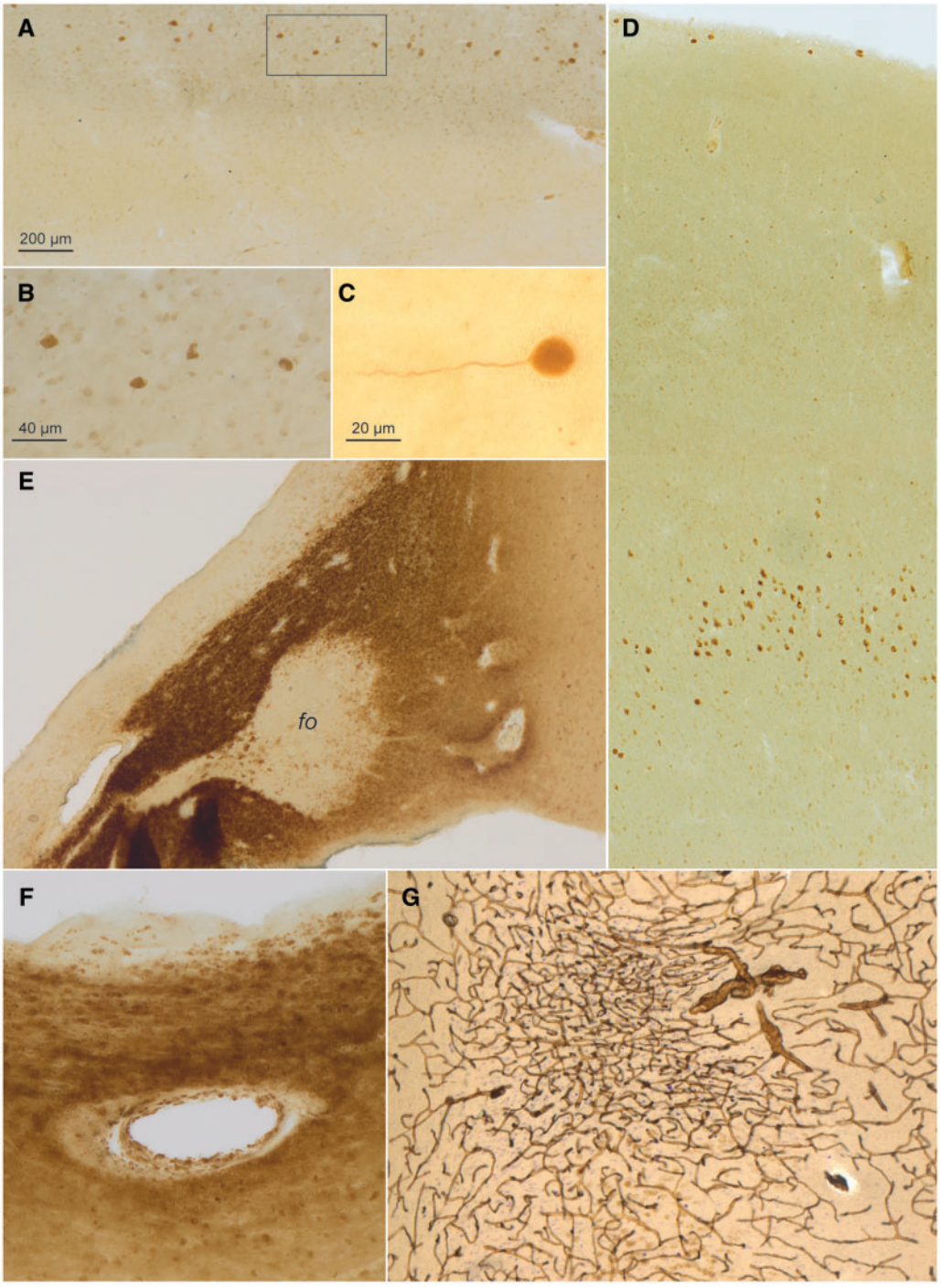

FIGURE 2. CD77-immunopositive intraneuronal inclusions (continued), CD77-immunopositive astrocytic and vascular inclusions in a 58-year-old male with Fabry disease. **(A)** Cajal-Retzius cells in layer I of the anterior cingulate gyrus contained Gb3 accumulations (DAB, brown chromogen). Framed area is shown at higher magnification in panel **(B)**. **(C)** Detail of SMI-311-immunopositive Cajal-Retzius cell in the molecular layer located between the dentate fascia and sector CA1 close to the obliterated hippocampal fissure. **(D)** Overview showing CD77-positive (DAB) pyramidal cells in layers I and Vb of the fusiform gyrus. **(E)** Intensely CD77-immunoreactive astrocytes in the hypothalamus and, to a considerably lesser extent, in the fornix (*fo*). **(F)** Gb3 (CD77) deposits (DAB, brown chromogen) in a vessel wall close to the lateral ventricle surrounded by intensely CD77-positive astrocytes. **(G)** Tortuous vessels and an infarction marked by puckering of the capillary network (collagen IV) in the subiculum (DAB, brown chromogen, plus erythrosin-phosphotungstic acid-aniline blue staining) (96). Immunoreactions: CD77 (DAB) or, in **(G)**, collagen IV with EPA staining in 100 µm sections. Scale bar in **(A)** applies to **(D)**, **(E)**, and **(G)**. Scale bar in **(B)** is also valid for **(F).**

TABLE 3. Regional Distribution and Severity of Fabry Disease Astrocytic CD77-Positive Gb3 Inclusions in 2 Cases

Case		1	2
olf	Olfactory bulb/tract	+++	+
dm	Dorsal motor nucleus of the glossopharyngeal and vagal nerves (IX/X)	++	+
ap	Area postrema	++	++
ge	Gelatinosus nucleus	++	NA
io	Inferior olivary complex	+	+
fL	Subependyma close to the foramen of Luschka (fourth ventricle)	+++	NA
ts	Subependyma along anterior horn of lateral ventricle, medially from bed nucleus of the terminal stria	+++	NA
fo	Fornix	++	NA
CA1	Alveus of CA1	+++	++
ep	Subependyma along posterior horn of lateral ventricle	+++	−
pur	Bergman glia in the molecular and Purkinje cell layers of the cerebellum	+	−
vh	Spinal cord ventral horn α-motoneurons (layer 9)	+	NA
dh	Spinal cord dorsal horn (layers 1 and 2)	+	NA

The pathology was assessed semiquantitatively: −, absent or not detectable; +, slight; ++, moderate; +++, severe. Only regions with CD77-positivity are shown. For accompanying heat map, see Supplementary Data Table.
NA, not available.

the cerebral cortex were α-synuclein-positive. Of the thalamic nuclei, only the intralaminar nuclei were mildly involved (84) (Table 4).

Although the nerve cells of the pallidum and claustrum were free of pathology, the putamen displayed both α-synuclein-positive punctate inclusions and strongly α-synuclein-positive astrocytes (106) (Table 4).

In the CA2 sector of the hippocampal formation, slender Lewy neurites were visible; these were accompanied by the presence of a few LBs in the pre-α layer of the transentorhinal region and in the deep layers of the entorhinal cortex (pri-α and pri-γ) (Table 4). Cajal-Retzius cells in the hippocampal formation and in additional brain regions were α-synuclein-immunonegative. Slight affection was present both in the superficial and deep layers of the limbic prepiriform cortex (Table 4; Fig. 1A). LP was not found in the neocortex or cerebellum of this patient. Layer Vb pyramidal cells in the anterior cingulate gyrus and agranular insula displayed mild involvement (Table 4).

Sparse LP existed in the anterolateral funiculus, layer I of the dorsal horn, and intermediolateral nucleus of the thoracic spinal cord (107–109) (Table 4). The dorsal root ganglia, which become involved in Lewy body disease (108, 109), were unavailable for assessment.

Finally, although seldom, LP and Gb3 accumulations were observed in one and the same nerve cell (4) in the dorsal motor nucleus of the vagal nerve, motor nucleus of the facial nerve, and dorsal raphe nucleus (Fig. 4D, E).

DISCUSSION

Although tissue from a smaller number of regions was available from the second FD patient and the severity of the CD77-immunoreactive inclusions showed some interpatient variation, the regional distribution patterns of the deposits in both individuals were generally similar (see Supplementary Data Tables for heat maps accompanying Tables 2–4). Our findings differed from those of Askari et al (54), who reported that intraneuronal Gb3 inclusions were confined only to the parahippocampal gyrus, and from the claim by Kaye et al (51) that "nearly all of the cerebral cortex" remain unaffected. Instead, our findings in cortical regions were somewhat more in agreement with those of deVeber et al (53). At the same time, it should be borne in mind that many of the early morphological studies were not based primarily on immunocytochemistry but mostly on Luxol fast blue staining, which visualizes sphingomyelin (47, 49, 50, 63). Here, neocortical CD77-positive intraneuronal pathology was chiefly confined to the insula and temporal lobe.

We could corroborate many of the previous findings of Gb3 intraneuronal accumulations in FD reported by other groups in nerve cells of the glossopharyngeus-vagus nuclear complex, in nuclei of the serotonergic lower and upper raphe groups, the central reticular nucleus of the pons, spinal tract nucleus of the trigeminal nerve, in the substantia nigra pars reticulata, the basal nucleus of the amygdala, inferior temporal gyrus and agranular insular cortex, hypothalamic supraoptic and paraventricular nuclei, portions of the spinal cord (47, 49–51, 53, 56), in cerebral vessel walls (46, 49–51, 53, 63, 100), as well as the astrocytic involvement in brain regions with direct contact to the ventricular system and subarachnoidal space (46, 50, 51). In contrast to previous studies (46, 49, 53), we saw no Gb3 accumulation in neuromelanin-containing neurons of the substantia nigra pars compacta (A9 group), in the presubiculum (50, 51), subiculum (53), or visual cortex ("calcarine cortex" [51]) except for Cajal-Retzius cell in layer I.

Regions assessed here with neurons not previously known to be involved in FD were the prepositus nucleus of the hypoglossal nerve, the motor nucleus of the facial nerve, the pigmented parabrachial nucleus, cortical accessory nucleus of the amygdala, basal nucleus of Meynert, bed nucleus of the diagonal band, bed nucleus of the terminal stria, prosubiculum, transentorhinal cortex (layer pri-β), and the prepiriform cortex.

Contrary to all earlier neuropathological studies of FD that lacked the olfactory bulb, astrocytic involvement of the olfactory tract in both patients was seen, and, whereas hyposmia in pure FD has not been reported previously (77), there is reason to believe that the FD patient without LP but with severe Gb3 lesions in the cortical accessory (olfactory) nucleus of the amygdala and the patient with olfactory bulb LP and CD77 lesions in the prepiriform cortex as well as in the cortical accessory nucleus of the amygdala would have displayed smell deficits, had they undergone olfactory testing.

In the individual with concomitant FD and LP, additional novel findings were the CD77 immunostaining seen in the persisting Cajal-Retzius cells (98, 110) of the molecular layer between the dentate fascia and Ammon's horn, in the agranular insula, and, generally, in the primary visual neocortex, on the dorsal aspect of the corpus callosum, and throughout the neocortex in layer I. Most sphingolipidoses, and

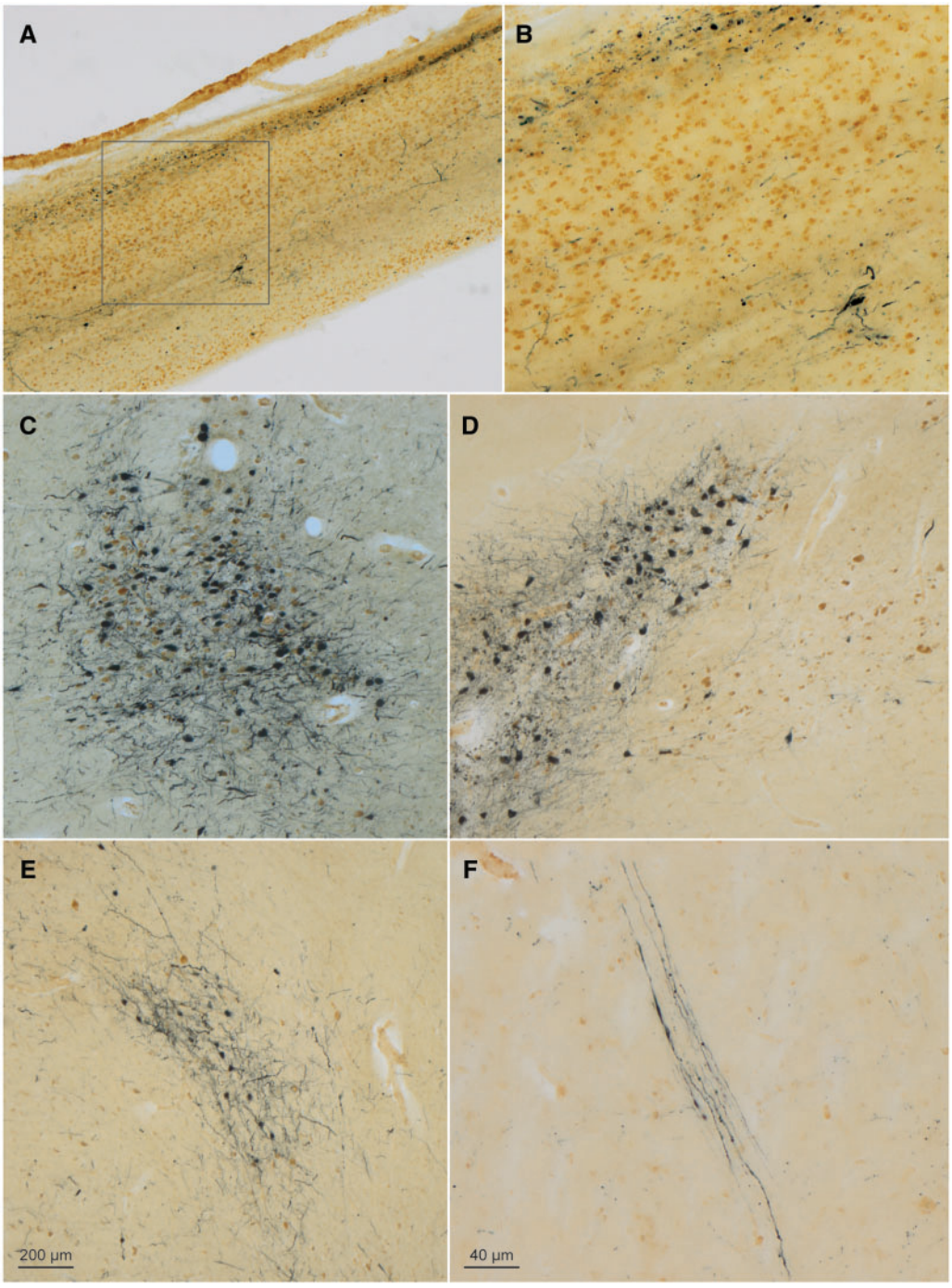

FIGURE 3. α-Synuclein-immunopositive Lewy neurites and Lewy bodies in a 58-year-old male with Fabry disease. **(A)** In the olfactory bulb, syn-1 immunoreactive LP (SK-4700, dark blue chromogen) occurred in the olfactory tract and anterior olfactory nucleus, and numerous CD77-positive (DAB, brown chromogen) astrocytes were present. Framed area is shown at higher magnification in panel **(B)**. **(C)** Micrograph of LP and cell loss in the locus coeruleus. **(D)** LP (SK-4700) accompanied by very severe cell loss in the pars compacta of the substantia nigra (at left); noncatecholaminergic nerve cells within the paranigral nucleus (at right) were CD77-immunopositive (DAB) and accompanied by fewer LP-containing catecholaminergic neurons than the pars compacta. **(E)** Lewy bodies/neurites (SK-4700) in the somatomotor system tegmental pedunculopontine nucleus. **(F)** LP (SK-4700) in axons of the vagal nerve in the medulla oblongata (intermediate reticular zone), a finding identical to that seen in the medulla of individuals with Parkinson's disease. Immunoreactions: CD77 or CD77 plus syn-1 in 100 µm sections. Scale bar in **(E)** applies to **(A)**, **(C)**, and **(D)**. Scale bar in **(F)** is also valid for **(B)**.

TABLE 4. Regional Distribution and Severity of Lewy Pathology in a Case With Fabry Disease

Case		1	2
aon/ob	Anterior olfactory nucleus and olfactory tract/ olfactory bulb	+++/++	−
dm	Dorsal motor nucleus of the vagal nerve (X)	++	−
ap	Area postrema	+	−
irz	Intermediate reticular zone	++	−
ro	Obscure raphe nucleus	+	−
rm	Great raphe nucleus	++	NA
gig	Gigantocellular nucleus of the reticular formation	++	NA
ph	Prepositus hypoglossal nucleus	++	NA
fa	Motor nucleus of the facial nerve (VII)	+	NA
tr	Spinal tract nucleus of the trigeminal nerve	+	NA
lc	Locus coeruleus	+++	−
pc	Central reticular nucleus of the pons	+	−
dr	Dorsal raphe nucleus	+++	−
cr	Central raphe nucleus	+	−
sn	Substantia nigra, pars compacta	+++	−
pa	Paranigral nucleus	+	NA
pg	Pigmented parabrachial nucleus	++	NA
ppt	Pedunculopontine tegmental nucleus	+++	−
oc	Oculomotor nucleus (III)	+	NA
ce	Central nucleus of the amygdala	+	−
ba	Basal nucleus of the amygdala	+	−
la	Lateral nucleus of the amygdala	+	−
ct	Cortical nucleus of the amygdala	+	NA
ac	Accessory cortical nucleus of the amygdala	++	−
me	Medial nucleus of the amygdala	+	−
db	Interstitial nucleus of the diagonal band	++	−
bn	Basal nucleus of Meynert	++	NA
so	Hypothalamic supraoptic nucleus	+	−
pv	Hypothalamic paraventricular nucleus	+	NA
tm	Hypothalamic tuberomamillary nucleus	++	NA
tl	Hypothalamic lateral tuberal nucleus	+	NA
in	Thalamic intralaminar nuclei	+	NA
rt	Reticular nucleus of the thalamus	+	NA
pu	Putamen	+++	−
nc	Caudate nucleus	++	NA
CA2	Ammon's horn, second sector	+	−
tre	Transentorhinal cortex	+	−
ent	Entorhinal cortex	+	−
pi	Prepiriform cortex (Brodmann Area 51)	+	NA
ai	Agranular insular cortex, layer Vb	+	NA
ci	Anterior cingulate gyrus, layer Vb	+	NA
af	Anterolateral funiculus of the spinal cord	+	NA
lam 1	Layer 1 of the spinal cord	+	NA
IML	Intermediolateral nucleus (layer 7) of the spinal cord	+	NA

The pathology was assessed semiquantitatively: − absent or not detectable; + slight; ++ moderate; +++ severe. Only regions that displayed Lewy pathology are shown. For accompanying heat maps, see Supplementary Data Tables.
NA, not available.

lysosomal storage diseases in general, can be characterized by central nervous system involvement, including early developmental delay. Thus, the involvement of persisting Cajal-Retzius cells in FD might be a remnant of or reflect some degree of abnormal central nervous system development.

Notably, in contradistinction to the findings in GD by Wong et al (14), whose study cohort included 14 autopsy brains, the sectors CA2-4, layer III of the cerebral cortex, and layer IVb of Brodmann Area 17 were not selectively involved in FD. Rather, it was the prosubiculum of both patients that displayed changes in the form of severe CD77-immunoreactivity of pyramidal cells (Table 2). Furthermore, the astrocytic and vascular inclusions seen here in FD do not find their counterparts in human GD (72). Thus, the distribution of the Gb3 inclusions in FD differs from the glucocerobrosidase immunoreactivity seen in GD (31); yet, like GD, the neuropathology in FD is remarkably selective (as pointed out earlier by others) (14, 49, 51, 53) despite the ongoing lack of a cogent explanation for the predilection of the intraneuronal inclusions for autonomic and limbic portions of the central nervous system (51, but see also 53). Moreover, although hyposmia/anosmia, as found in individuals with *GBA1* mutations (111, 112), were not tested for in the patient with FD and LP, our present findings indicate that olfactory regions also become involved during FD. The same was true, to a lesser extent, of motor nuclei of the lower brainstem. The involvement of the prepiriform cortex in FD is remarkable inasmuch as the connectivity of this area points to a close linkage between the olfactory and limbic systems.

The fact that CD77-positive nerve cells were seen directly nearby CD77-negative nerve cells within involved regions indicates that the Gb3 pathology does not spread contiguously between neurons in FD but, if at all, possibly along a diffusion gradient across the blood-brain barrier (113), where CD77-positive astrocytes may act as 'carriers.' In the FD patient with coincident LP, it was notable that the intramedullary axons of the dorsal motor nucleus of the vagal nerve displayed greater α-synuclein involvement than the preganglionic visceromotor neurons within the parent nucleus itself. These ballooned nerve cells, in turn, were completely filled and perhaps thereby 'overcrowded' with Gb3 inclusions (compare Fig. 1B and Figs. 3F and 4F). This might possibly mean that the LP within the axons of the vagal nerve could have originated elsewhere and been transported retrogradely to the dorsal motor nucleus, where LP was unable to 'displace' the Gb3 deposits already filling or 'occupying' the large visceromotor nerve cells of the dorsal motor nucleus.

Some authors have speculated that the pathomechanistic link between GD and Parkinson disease might well extend to other inherited lysosomal enzymopathies (114, 115). Epidemiological data confirming the co-occurrence and/or interaction of GD and Parkinson disease are stronger than the data currently available for FD and Parkinson disease (72). Nevertheless, the results from 3 recent studies provide new evidence clearly linking FD and Parkinson disease. Briefly, in an MRI-based study, it was seen that, when compared to controls, FD patients (n = 30) who had undergone clinical examination for motor functioning displayed significantly reduced nigral volumes accompanied by significant increases in susceptibility values of the substantia nigra and striatum (116). In a second study, this time of the postmortem substantia nigra from 2

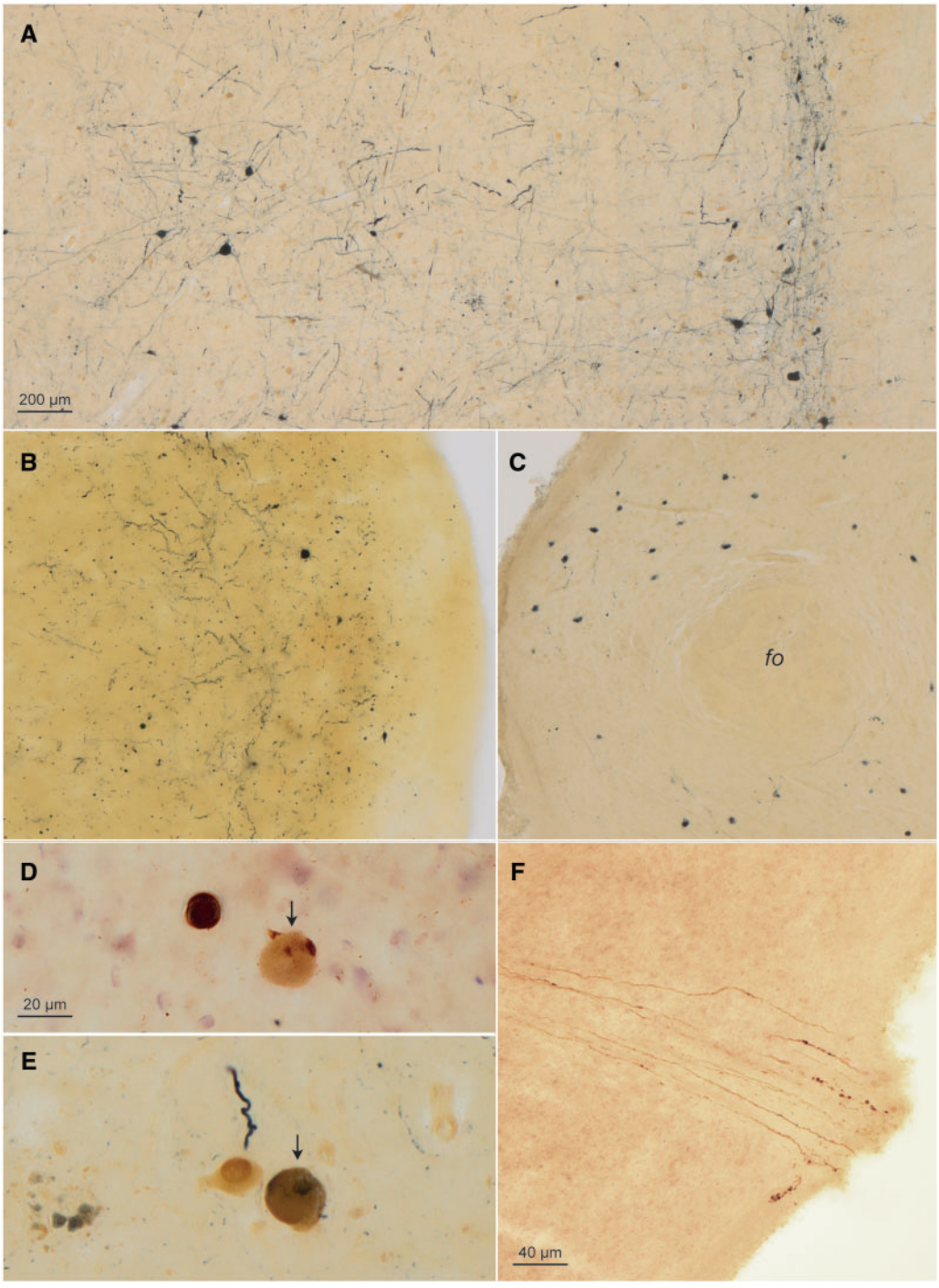

FIGURE 4. α-Synuclein-immunopositive Lewy neurites/bodies and CD77-immunopositive intraneuronal inclusions (continued) in a 58-year-old male Fabry patient. **(A)** The great raphe nucleus (at right) and gigantocellular reticular nucleus (at left): Gb2 inclusions (DAB, brown chromogen) and more numerous Lewy bodies/neurites (SK-4700, dark blue chromogen) in the reticular formation. **(B)** LP in the accessory cortical (olfactory) nucleus of the amygdala. **(C)** LP in the tuberomamillary nucleus of the hypothalamus (*fo*, fornix). **(D, E)** Isolated ballooned CD77-immunopositive nerve cells were also syn-1-positive, for example, here, in the dorsal motor nucleus of the vagal nerve (arrow in **D**, compare the Lewy body at left) and in a motoneuron in the motor nucleus of the facial nerve (arrow in **E**, compare the Lewy neurite and CD77-positive cell at left). In micrograph **E**, syn-1-positive extraneuronal remnants faintly positive for CD77 (lower left) mark the place where cell loss has occurred. **(F)** Note the syn-1 (here, DAB)-immunoreactive axons of the medullary portion of the vagal nerve at the point where axons exit the lower brainstem (lower right) to the periphery. Immunoreactions: Syn-1 except for micrographs **(A)**, **(D)**, and **(E)** (CD77 plus syn-1 double immunohistochemistry) in 100 µm sections. Scale bar in **(A)** applies to **(C)**. Scale bar in **(F)** is also valid for **(B)**; bar in **(D)** applies to **(E)**.

independent Parkinson disease cohorts (n = 18 and n = 20) in which all cases were neuropathologically staged for Parkinson disease, Huebecker et al (117) established an association between sporadic Parkinson disease and deficiencies that reached significance in several lysosomal hydrolases, including α-Gal A, in comparison to age- and gender-matched controls. The authors found no significant statistical differences between 4 Parkinson patients with *GBA* mutations and the remaining sporadic Parkinson disease individuals, who lacked *GBA* mutations (117). A third relevant study determined the prevalence of Parkinson disease in a large FD cohort (n = 229) consisting of 31 Portuguese families carrying a single *GLA* gene mutation to be 3% in patients ≥50 years of age (118). While screening for major known Parkinson disease genes did not identify *SNCA* duplications or triplications in this cohort, we anticipate that, provided α-synuclein immunohistochemistry were to be performed (72), additional FD cases associated with sporadic Parkinson disease, as reported by Huebecker et al (117), may come to light in future autopsy-controlled FD studies.

Above, we used the term "Lewy body pathology" to describe α-synuclein-positive lesions in the brain and spinal cord sections of the 58-year-old Fabry patient. Assessment of collagen IV immunoreactions showed the presence of 3 small infarcts (Fig. 2F) but not that of diffuse severe white matter lesions (103, 119), multiple widespread cortical or subcortical microinfarcts, that is, morphological substrates suggestive of vascular-induced parkinsonism (120). Staining for Aβ did not reveal the existence of cortical amyloid angiopathy. Moreover, as revealed by AT8 and TDP-43 immunohistochemistry, parkinsonism in this individual could not be attributed to an 'atypical' parkinsonian syndrome, such as progressive supranuclear palsy, or other frontotemporal lobar degeneration subtypes (121–123). Finally, the patient's hypokinesia was unaccompanied by cognitive impairment or by manifestations typically associated with DLB, such as recurrent hallucinations or fluctuating cognition (105), whereas α-synuclein immunohistochemistry showed a regional distribution pattern of LP compatible with neuropathological stage 4 of Parkinson disease (84, 85, 106) (Table 4).

For these reasons, we conclude that this FD patient with parkinsonism and nigral cell loss had also suffered from the synucleinopathy Parkinson disease, a heretofore unknown co-occurrence in FD (77, 114). In this context, it is also noteworthy that LP has been described in brains from patients with concomitant GD and Parkinson disease but not in brains of individuals with GD without parkinsonism (14). Similarly, here, LP existed in the brain of a patient with FD and with Parkinson disease but not in another 'control' FD patient without clinical parkinsonism (Tables 1, 4). That the first patient's hypokinesia—which is consistent with the existence of LP and severe neuronal loss in the substantia nigra compounded by prominent involvement of the locus coeruleus and somatomotor system tegmental pedunculopontine nucleus (84, 124)—was not a major focus of his clinicians' attention and not followed up by a referral to a movement disorders specialist, can be partially explained by the fact that the symptom was first noted near the end of his life. After the initial manifestation of FD in early adolescence, the patient's clinical history had been dominated for more than 25 years by increasingly severe cardiac and renal complications.

This study was constrained by the unavailability of (1) tissue samples from the enteric or peripheral nervous system and (2) extensive tissue samples from all levels of the spinal cord from both FD cases, (3) the small FD sample size evaluated, and (4) a lack of knowledge about the *GLA* variants in both individuals (36–38). However, nearly all older neuropathological studies of FD cited herein were also performed on small cohorts or on single cases (47, 49, 51, 53, 63, 100), and the FD diagnosis in the 58-year-old patient was confirmed at autopsy based on ultrastructural evidence and neuropathological examination, so that a cardiac variant of FD without involvement of the vascular endothelium could definitely be excluded (79, 125, 126).

In closing, parkinsonism accompanied by LP can occur in FD. Additional multicenter studies involving substantially larger autopsy-controlled FD cohorts that also include females (43, 103) are needed to determine the frequency and full extent of both phenomena within the human nervous system as well as how both pathologies, including that seen in astrocytes (127), might interact in comparison to the interactions that have been proposed for GD (128–132). Such studies could indicate whether FD with LP is associated with a late- versus early-onset of Lewy body disease-related symptoms and a more or less aggressive disease course, and whether the lesions seen here in autonomic centers could correlate with possible symptoms in FD, similar to the autonomic dysfunction reported in GD-associated Parkinson disease (133). In GD, *GBA1* mutations may trigger α-synuclein aggregation directly (15) or they may enhance it (134); however, it is not known whether the same could be true in FD. With suitable models and novel methods (135, 136), it may become possible to understand the implications of both types of lesions for disease pathogenesis, potential spreading mechanisms (51, 137), and improved therapeutic interventions for both multisystem disorders.

ACKNOWLEDGMENTS

The authors wish to thank Mr. David Ewert (University of Ulm) for skillful technical assistance (figure layout). The authors also wish to express their sincere thanks to Mr. John Cottrell for human tissue obtained from the NIH Neurobiobank at the University of Maryland, Baltimore, MD (https://neurobiobank.nih.gov). In memoriam: Rev. Gerard H. Ettlinger, S.J. (1935-2018).

REFERENCES

1. Hruska KS, LaMarca ME, Scott CR, et al. Gaucher disease: Mutation and polymorphism spectrum in the glucocerebrosidase gene (GBA). Hum Mutat 2008;29:567–83
2. Neudorfer O, Giladi N, Elstein D, et al. Occurrence of Parkinson's syndrome in type I Gaucher disease. QJM 1996;89:691–4
3. Goker-Alpan O, Giasson BI, Eblan MJ, et al. Glucocerebrosidase mutations are an important risk factor for Lewy body disorders. Neurology 2006;67:908–10
4. Goker-Alpan O, Stubblefield BK, Giasson BI, et al. Glucocerebrosidase is present in α-synuclein inclusions in Lewy body disorders. Acta Neuropathol 2010;120:641–9

5. Farrer MJ, Williams LN, Algom AA, et al. Glucosidase-beta variations and Lewy body disorders. Parkinsonism Relat Disord 2009; 15:414–6
6. Neumann J, Bras J, Deas E, et al. Glucocerebrosidase mutations in clinical and pathologically proven Parkinson's disease. Brain 2009;132: 1783–94
7. Sidransky E, Nalls MA, Aasly JO, et al. Multicenter analysis of glucocerebrosidase mutations in Parkinson's disease. N Engl J Med 2009; 361:1651–61
8. Hardy J. Genetic pathways to Parkinson disease. Neuron 2010;68: 201–6
9. Nishioka K, Ross OA, Vilariño-Güell C, et al. Glucocerebrosidase mutations in diffuse Lewy body disease. Parkinsonism Relat Disord 2011;17:55–7
10. Nalls MA, Duran R, Lopez G, et al. A multicenter study of glucocerebrosidase mutations in dementia with Lewy bodies. JAMA Neurol 2013;70:727–35
11. Robak LA, Jansen IE, van Rooij J, et al.; International Parkinson's Disease Genomics Consortium (IPDGC). Excessive burden of lysosomal storage disorder gene variants in Parkinson's disease. Brain 2017;140: 3191–203
12. Mullin S, Hughes D, Mehta A, et al. Neurological effects of glucocerebrosidase gene mutations. Eur J Neurol 2019;26:388–93
13. Bembi B, Zambito Marsala S, Sidranksy E, et al. Gaucher's disease with Parkinson's disease: Clinical and pathological aspects. Neurology 2003;61:99–101
14. Wong K, Sidransky E, Verma A, et al. Neuropathology provides clues to the pathophysiology of Gaucher disease. Mol Genet Metab 2004;82: 192–207
15. Westbroek W, Gustafson EM, Sidransky E. Exploring the link between glucocerebrosidase mutations and parkinsonism. Trends Mol Med 2011;17:485–93
16. Li Y, Li P, Liang H, et al. Gaucher-associated parkinsonism. Cell Mol Neurobiol 2015;35:755–61
17. Balestrino R, Schapira A. Glucocerebrosidase and Parkinson disease: Molecular, clinical, and therapeutic implications. Neuroscientist 2018; 24:540–59
18. Blandini F, Cilia R, Cerr S, et al. Glucocerebrosidase mutations and synucleinopathies: Toward a model of precision medicine. Mov Disord 2019;34:9–21
19. Gatto EM, Da Prat G, Etcheverry JL, et al. Parkinsonisms and glucocerebrosidase deficiency: A comprehensive review for molecular and cellular mechanism of glucocerebrosidase deficiency. Brain Sci 2019;9: pii: E30
20. Anderson W. A case of "angeio-keratoma." Br J Dermatol 1898;10: 113–7
21. Fabry J. Ein Beitrag zur Kenntniss der Purpura haemorrhagica nodularis (Purpura papulosa haemorrhagica Hebrae). Arch f Dermat 1898;43: 187–200
22. van Andel P. Angiokeratoma corporis diffusum (Fabry's diseases). Dermatologica 1974;148:48–9
23. Miller JJ, Kanack AJ, Dahms NM. Progress in the understanding and treatment of Fabry's disease. Biochim Biophys Acta Gen Subj 2020; 1864:129437
24. Opitz JM, Stiles FC, Wise D, et al. The genetics of angiokeratoma corporis diffusum (Fabry's disease) and its linkage relations with the Xg locus. Am J Hum Genet 1965;17:325–45
25. Kaminsky P, Noel E, Jaussaud R, et al. Multidimensional analysis of clinical symptoms in patients with Fabry's disease. Int J Clin Pract 2013;67:120–7
26. Kint JA. Fabry's disease: Alpha-galactosidase deficiency. Science 1970;167:1268–9
27. Desnick RJ, Ioannou YA, Eng CM. α-Galactosidase A deficiency: Fabry disease. In: Scriver CR, Beaudet AL, Sly WS, Valle D, Kinzler KE, Vogelstein B, eds. The Metabolic and Molecular Bases of Inherited Disease, 8th edn. New York: McGraw-Hill 2001:3733–74
28. Germain DP. Fabry disease. Orphanet J Rare Dis 2010;5:30
29. Gal A, Beck M, Höppner W, et al. Clinical utility gene card for: Fabry disease – update 2016. Eur J Hum Genet 2017;25:e1–e3
30. Sachdev B, Takenaka T, Teraguchi H, et al. Prevalence of Anderson-Fabry disease in male patients with late onset hypertrophic cardiomyopathy. Circulation 2002;105:1407–11
31. Rolfs A, Böttcher T, Zschiesche M, et al. Prevalence of Fabry disease in patients with cryptogenic stroke: A prospective study. Lancet 2005;366: 1794–6
32. Hoffmann B, Mayatepek E. Fabry disease – often seen, rarely diagnosed. Dtsch Arztebl Int 2009;106:440–7
33. Mechtler TP, Stary S, Metz TF, et al. Neonatal screening for lysosomal storage disorders: Feasibility and incidence from a nationwide study in Austria. Lancet 2012;379:335–41
34. Laney DA, Bennett RL, Clarke V, et al. Fabry disease practice guidelines: Recommendations of the National Society of Genetic Counselors. J Genet Counsel 2013;22:555–64
35. Hwu WL, Chien YH, Lee NC, et al. Newborn screening for Fabry disease in Taiwan reveals a high incidence of the later-onset mutation c.936 + 919G>A (IVS4 + 919G>A). Hum Mutat 2009;30:1397–405
36. Van der Tol L, Smid BE, Poorthuis B, et al. A systematic review on screening for Fabry disease: Prevalence of individuals with genetic variants of unknown significance. J Med Genet 2014;51:1–9
37. Smid BE, Van der Tol L, Cecchi F, et al. Uncertain diagnosis of Fabry disease: Consensus recommendation on diagnosis in adults with left ventricular hypertrophy and genetic variants of unknown significance. Int J Cardiol 2014;177:400–8
38. Ortiz A, Germain DP, Desnick RJ, et al. Fabry disease revisited: Management and treatment recommendations for adult patients. Mol Genet Metab 2018;123:416–27
39. Caudron E, Prognon P, Germain DP. Enzymatic diagnosis of Fabry disease using a fluorometric assay on dried blood spots: An alternative methodology. Eur J Med Genet 2015;58:681–4
40. Desnick RJ, Brady R, Barranger J, et al. Fabry disease, an underrecognized multisystemic disorder: Expert recommendations for diagnosis, management, and enzyme replacement therapy. Ann Intern Med 2003;138:338–46
41. Desnick RJ, Schuchman EH. Enzyme replacement therapy for lysosomal diseases: Lessons from 20 years of experience and remaining challenges. Annu Rev Genom Hum Genet 2012;13:307–35
42. Germain DP, Charrow J, Desnick RJ, et al. Ten-year outcome of enzyme replacement therapy with agalsidase beta in patients with Fabry disease. J Med Genet 2015;52:353–8
43. MacDermot KD, Holmes A, Miners AH. Anderson-Fabry disease: Clinical manifestations and impact of disease in a cohort of 60 obligate carrier females. J Med Genet 2001;38:769–75
44. Citro V, Cammisa M, Liguori L, et al. The large phenotypic spectrum of Fabry disease requires graduated diagnosis and personalized therapy: A meta-analysis can help to differentiate missense mutations. Int J Mol Sci 2016;17:pii: E2010
45. Pompen AW, Ruiter M, Wyers HJ. Angiokeratoma corporis diffusum (universale) Fabry, as a sign of an unknown internal disease; two autopsy reports. Acta Med Scand 2009;128:234–55
46. Rahman AN, Lindenberg R. The neuropathology of hereditary dystopic lipidosis. Arch Neurol 1963;9:373–85
47. Schibanoff JM, Kamoshita S, O'Brien JS. Tissue distribution of glycosphingolipids in a case of Fabry's disease. J Lipid Res 1969;10:515–20
48. Rowe JW, Gillian JI, Worthin TA. Intestinal manifestations of Fabry's disease. Ann Intern Med 1974;81:628–30
49. Kahn P. Anderson-Fabry disease: A histopathological study of three cases with observations on the mechanism of production of pain. J Neurol Neurosurg Psychiatry 1973;36:1053–62
50. Tabira T, Goto I, Kuroiwa Y, et al. Neuropathological and biochemical studies in Fabry's disease. Acta Neuropathol 1974;30:345–54
51. Kaye EM, Kolodny EH, Logigian EL, et al. Nervous system involvement in Fabry's disease: Clinicopathological and biochemical correlation. Ann Neurol 1988;23:505–9
52. Jack CI, Morris AI, Nasmyth DG, et al. Colonic involvement in Fabry's disease. Postgrad Med J 1991;67:584–5
53. deVeber GA, Schwarting GA, Kolodny EH. Fabry disease: Immunocytochemical characterization of neuronal involvement. Ann Neurol 1992;31:409–15
54. Askari H, Kaneski CR, Semino-Mora C, et al. Cellular and tissue localization of globotriaosylceramide in Fabry disease. Virchows Arch 2007; 451:823–34
55. Scriba K. Zur Pathogenese des Angiokeratoma corporis diffusum Fabry mit kardio-vaso-renalem Symptomenkomplex. Verh Dtsch Path Ges 1950;34:221–6

56. Steward VW, Hitchcock C. Fabry's disease (angiokeratoma corporis diffusum). A report of 5 cases with pain in the extremities as the chief symptom. Pathol Eur 1968;3:377–88
57. Gadoth N, Sandbank U. Involvement of dorsal root ganglia in Fabry's disease. J Med Genet 1983;20:309–12
58. Tagliavini F, Pietrini V, Gemignani F, et al. Anderson-Fabry's disease: Neuropathological and neurochemical investigation. Acta Neuropathol 1982;56:93–8
59. Tuppurainen K, Collan Y, Rantanen T, et al. Fabry's disease and cornea verticillata. A report of 3 cases. Acta Ophthalmol (Copenh) 1981;59: 674–82
60. Sestito S, Ceravolo F, Concolino D. Anderson-Fabry disease in children. Curr Pharm Dis 2013;19:6037–45
61. Politei J, Thurberg EL, Wallace E, et al. Gastrointestinal involvement in Fabry disease. So important, yet often neglected. Clin Genet 2016;89: 5–9
62. Politei J, Durand C, Schenone AB, et al. Chronic intestinal pseudoobstruction. Did you search for lysosomal storage diseases? Mol Genet Metab Rep 2017;11:8–11
63. Reske-Nielsen E, Lou HO. Neuropathological studies in Fabry's disease. Acta Neurol Scand 1970;46(Suppl 43):259–60
64. MacDermot KD, Holmes A, Miners AH. Anderson-Fabry disease: Clinical manifestations and impact of disease in a cohort of 98 hemizygous males. J Med Genet 2001;38:750–60
65. Sims K, Politei J, Banikazemi M, et al. Stroke in Fabry disease frequently occurs before diagnosis and in the absence of other clinical events: Natural history data from the Fabry Registry. Stroke 2009;40: 788–94
66. Schermuly I, Müller MJ, Müller KM, et al. Neuropsychiatric symptoms and brain structural alterations in Fabry disease. Eur J Neurol 2011;18: 347–53
67. Bolsover FE, Murphy E, Cipolotti L, et al. Cognitive dysfunction and depression in Fabry disease: A systematic review. J Inherit Metab Dis 2014;37:177–87
68. Kolodny E, Fellgiebel A, Hilz MJ, et al. Cerebrovascular involvement in Fabry disease: Current status of knowledge. Stroke 2015;46:302–13
69. Nair V, Belanger EC, Veinot JP. Lysosomal storage disorders affecting the heart: A review. Cardiovasc Pathol 2019;39:12–24
70. Orimo S, Iwasaki T, Yoshino H. An autopsied case of Fabry's disease presenting with parkinsonism and cardiomegaly as a cardinal clinical manifestation. Rinsho Shinkeigaku 1994;34:1003–7
71. Buechner S, De Cristofaro MT, Ramat S, et al. Parkinsonism and Anderson Fabry's disease: A case report. Mov Disord 2006;21:103–7
72. Wise AH, Yang A, Naik H, et al. Parkinson's disease prevalence in Fabry disease: A survey study. Mol Genet Metab Rep 2018;14:27–30
73. Nelson MP, Boutin M, Tse TE, et al. The lysosomal enzyme alpha-Galactosidase A is deficient in Parkinson's disease brain in association with the pathologic accumulation of alpha-synuclein. Neurobiol Dis 2018;110:68–81
74. Nelson MP, Tse TE, O'Quinn DB, et al. Autophagy-lysosome pathway associated neuropathology and axonal degeneration in the brains of alpha-galactosidase A-deficient mice. Acta Neuropathol Commun 2014;2:20
75. Valbuena C, Leitão D, Carneiro F, et al. Immunohistochemical diagnosis of Fabry nephropathy and localisation of globotriaosylceramide deposits in paraffin-embedded kidney tissue sections. Virchows Arch 2012;460:211–21
76. Linhart A, Elliott PM. The heart in Anderson-Fabry disease and other lysosomal storage disorders. Heart 2007;93:528–35
77. Löhle M, Hughes D, Milligan H, et al. Clinical prodromes of neurodegeneration in Anderson-Fabry disease. Neurology 2015;84:1454–64
78. Benjamin IJ, Schuster EH, Bulkley BH. Cardiac hypertrophy in idiopathic dilated congestive cardiomyopathy: A clinicopathologic study. Circulation 1981;64:442–7
79. Frustaci A, Chimenti C, Ricci R, et al. Improvement in cardiac function in the cardiac variant of Fabry's disease with galactose-infusion therapy. N Engl J Med 2001;345:25–32
80. Chang YH, Hwang SK. A case of cerebral aneurysmal subarachnoid hemorrhage in Fabry's disease. J Korean Neurosurg Soc 2013;53:187–9
81. Hughes DA, Nicholls K, Shankar SP, et al. Oral pharmacological chaperone migalastat compared with enzyme replacement therapy in Fabry disease: 18-month results from the randomised phase III ATTRACT study. J Med Genet 2017;54:288–96
82. Braak H, Braak E. Demonstration of amyloid deposits and neurofibrillary changes in whole brain sections. Brain Pathol 1991;1:213–6
83. Hyman BT, Phelps CH, Beach TG, et al. National Institute on Aging Alzheimer's Association guidelines for the neuropathologic assessment of Alzheimer's disease. Alzheimers Dement 2012;8:1–13
84. Braak H, Del Tredici K. Neuropathology and pathology of sporadic Parkinson's disease. Adv Anat Embryol Cell Biol 2009;201:1–119
85. Braak H, Del Tredici K, Rüb U, et al. Staging of brain pathology related to sporadic Parkinson's disease. Neurobiol Aging 2003;24:197–211
86. Ghebremedhin E, Braak H, Braak E, et al. Improved method facilitates reliable APOE genotyping of genomic DNA extracted from formaldehyde-fixed pathology specimens. J Neurosci Methods 1998; 79:229–31
87. Corder E, Saunders A, Strittmatter W, et al. Gene dose of apolipoprotein E and type 4 allelle and the risk of Alzheimer's disease in late-onset families. Science 1993;261:921–3
88. Wenneberg AM, Tosakulwong N, Lesnick TG, et al. Association of apolipoprotein E ε4 with transactive response DNA-binding protein 43. JAMA Neurol 2018;75:1347–54
89. Singleton AB, Wharton A, O'Brien KK, et al. Clinical and neuropathological correlates of apolipoprotein E genotype in dementia with Lewy bodies. Dement Geriatr Cogn Disord 2002;14:167–75
90. Tsuang D, Leverenz JB, Lopez OL, et al. APOE epsilon4 increases risk for dementia in pure synucleinopathies. JAMA Neurol 2013;70:223–8
91. Bras J, Guerreiro R, Darwent L, et al. Genetic analysis implicates APOE, SNCA and suggests lysosomal dysfunction in the etiology of dementia with Lewy bodies. Hum Mol Genet 2014;23:6139–46
92. Smithson KG, MacVicar BA, Hatton G. Polyethylene glycol embedding: A technique compatible with immunocytochemistry, enzyme histochemistry, histofluorescence and intracellular staining. J Neurosci Methods 1983;7:27–41
93. Feldengut S, Del Tredici K, Braak H. Paraffin sections of 70-100 µm: A novel technique and its benefits for studying the nervous system. J Neurosci Methods 2013;215:241–4
94. Braak H. Architectonics as seen by lipofuscin stains. In: Jones EG, Peters A, eds. Cerebral Cortex. Cellular Components of the Cerebral Cortex, Vol. I. New York: Plenum Press 1984:59–104
95. Dickson DW, Ahmed Z, Algom AA, et al. Neuropathology of variants of progressive supranuclear palsy. Curr Opin Neurol 2010;23:394–400
96. Braak H, Feldengut S, Kassubek J, et al. Two histological methods for recognition and study of cortical microinfarcts in thick sections. Eur J Histochem 2018;62:2989
97. Tan RH, Shepherd CE, Kril JJ, et al. Classification of FTLD-TDP cases into pathological subtypes using antibodies against phosphorylated and non-phosphorylated TDP43. Acta Neuropathol Commun 2013;1:33
98. Ulfig N, Nickel J, Bohl J. Monoclonal antibodies SMI 311 and SMI 312 as tools to investigate the maturation of nerve cells and axonal patterns in human fetal brain. Cell Tissue Res 1998;291:433–43
99. Saper CB, Petito C. Correspondence of melanin-pigmented neurons in human brain with A1–A14 catecholamine cell groups. Brain 1982;105: 87–101
100. Lou HOC, Reske-Nielsen E. The central nervous system in Fabry's disease. Arch Neurol 1971;25:351–9
101. Bütti C, Santos M, Uppal N, et al. Von Economo neurons: Clinical and evolutionary perspectives. Cortex 2013;49:312–26
102. Mitsias P, Levine SR. Cerbrovascular complications of Fabry's disease. Ann Neurol 1996;40:8–17
103. Fellgiebel A, Müller MJ, Ginsberg L. CNS manifestations of Fabry's disease. Lancet Neurol 2006;5:791–5
104. Kosaka K, Tsuchiya K, Yoshimura M. Lewy body disease with and without dementia: A clinicopathological study of 35 cases. Clin Neuropathol 1998;7:299–305
105. McKeith IG, Boeve BF, Dickson DW, et al. Diagnosis and management of dementia with Lewy bodies: Fourth consensus report of the DLB Consortium. Neurology 2017;89:88–100
106. Braak H, Sastre M, Del Tredici K. Development of alpha-synuclein immunoreactive astrocytes in the forebrain parallels stages of intraneuronal pathology in sporadic Parkinson's disease. Acta Neuropathol 2007; 114:231–41

107. Braak H, Sastre M, Bohl JRE, et al. Parkinson's disease: Lesions in dorsal horn layer I, involvement of parasympathetic and sympathetic pre- and postganglionic neurons. Acta Neuropathol 2007;113:421–9
108. Del Tredici K, Braak H. Spinal cord lesions in sporadic Parkinson's disease. Acta Neuropathol 2012;124:643–64
109. Sumikura H, Takao M, Hatsuta H, et al. Distribution of α-synuclein in the spinal cord and dorsal root ganglia in an autopsy cohort of elderly persons. Acta Neuropathol Commun 2015;3:57
110. Martínez-Cerdeño V, Noctor SC. Cajal, Retzius, and Cajal-Retzius cells. Front Neuroanat 2014;8:48
111. McNeill R, Duran R, Proukakis C, et al. Hyposmia and cognitive impairment in Gaucher disease patients and carriers. Mov Disord 2012;27:526–32
112. Beavan M, McNeill A, Proukakis C, et al. Evolution of prodromal clinical markers of Parkinson disease in a GBA mutation positive cohort. JAMA Neurol 2015;72:201–8
113. Abbott NJ, Rönnbäck L, Hansson E. Astrocyte-endothelial interactions at the blood-brain barrier. Nat Rev Neurosci 2006;7:41–53
114. Shachar T, Lo Bianco C, Recchia A, et al. Lysosomal storage disorders and Parkinson's disease: Gaucher disease and beyond. Mov Disord 2011;26:1593–604
115. Futerman AH, Hardy J. Perspective: Finding common ground. Nature 2016;537:S160–1
116. Russo C, Pontillo G, Pisani A, et al. Striatonigral involvement in Fabry Disease: A quantitative and volumetric Magnetic Resonance Imaging study. Parkinsonism Relat Disord 2018;57:27–32
117. Huebecker M, Moloney EB, van der Spoel AC, et al. Reduced sphingolipid hydrolase activities, substrate accumulation and ganglioside decline in Parkinson's disease. Mol Neurodegener 2019;14:40
118. Gago MF, Azevedo O, Guimarães A, et al. Parkinson's disease and Fabry's disease: Clinical, biochemical and neuroimaging analysis of three pedigrees. J Parkinsons Dis 2020;10:141–152.
119. Köver S, Vergouwe M, Hollak CEM, et al. Development and clinical consequences of white matter lesions in Fabry disease: A systematic review. Mol Genet Metab 2018;125:205–16
120. Zijlmans JC, Daniel SE, Hughes AJ, et al. Clinicopathological investigation of vascular parkinsonism, including clinical criteria for diagnosis. Mov Disord 2004;19:630–40
121. Alonso-Canovas A, Katschnig P, Tucci A, et al. Atypical parkinsonism with apraxia and supranuclear gaze abnormalities in type 1 Gaucher disease. Expanding the spectrum: Case report and literature review. Mov Disord 2010;25:1506–9
122. Deutschländer AB, Ross OA, Dickson DW, et al. Atypical parkinsonian syndromes: A general neurologist's perspective. Eur J Neurol 2018;25:41–58
123. Forrest SL, Crockford DR, Sizemova A, et al. Coexisting Lewy body disease and clinical parkinsonism in frontotemporal lobar degeneration. Neurology 2019;92:e2472–82
124. Benarroch EE. Pedunculopontine nucleus: Functional organization and clinical implications. Neurology 2013;80:1148–55
125. Chimenti C, Pieroni M, Morgante E, et al. Prevalence of Fabry disease in female patients with late-onset hypertrophic cardiomyopathy. Circulation 2004;110:1047–53
126. von Scheidt W, Eng CM, Fitzmaurice TF, et al. An atypical variant of Fabry's disease with manifestations confined to the myocardium. N Engl J Med 1991;324:395–9
127. Sorrentino ZA, Giasson BI, Chakrabarty P. α-Synuclein and astrocytes: Tracing the pathways from homeostasis to neurodegeneration in Lewy body disease. Acta Neuropathol 2019;138:1–21
128. Goldin E. Gaucher disease and parkinsonism, a molecular link theory. Mol Genet Metab 2010;101:307–10
129. Mazzulli JR, Xu YH, Sun Y, et al. Gaucher disease glucocerebrosidase and α-synuclein form a bidirectional pathogenic loop in synucleinopathies. Cell 2011;146:37–52
130. Bieri G, Brahic M, Bousset L, et al. LRRK2 modifies α-syn pathology and spread in mouse models and human neurons. Acta Neuropathol 2019;137:961–80
131. Zunke F, Moise AC, Belur NR, et al. Reversible conformational conversion of alpha-Synuclein into toxic assemblies by glucosylceramide. Neuron 2018;97:92–107.e10
132. Isacson O, Brekk OR, Hallett PJ. Novel results and concepts emerging from lipid cell biology relevant to degenerative brain aging and disease. Front Neurol 2019;10:1053
133. Brockmann K, Srulijes K, Hauser A-K, et al. GBA-associated PD presents with nonmotor characteristics. Neurology 2011;77:276–80
134. Goedert M. Neurodegeneration. Alzheimer's and Parkinson's diseases: The prion concept in relation to assembled Aβ, tau, and α-synuclein. Science 349:1255555
135. Kaneski CR, Brady RO, Hanover JA, et al. Development of a model system for neuronal dysfunction in Fabry disease. Mol Genet Metab 2016;119:144–50
136. Shahmoradian SH, Lewis AJ, Genoud C, et al. Lewy pathology in Parkinson's disease consists of crowded organelles and lipid membranes. Nat Neurosci 2019;22:1099–109
137. Karpowicz RJ, Haney CM, Mihaila TS, et al. Selective imaging of internalized proteopathic α-synuclein seeds in primary neurons reveals mechanistic insight into transmission of synucleinopathies. J Biol Chem 2017;292:13482–97
138. Hsu T-R, Sung S-H, Chang F-P, et al. Endomyocardial biopsies in patients with left ventricular hypertrophy and a common Chinese later-onset Fabry mutation (IVS4 + 919G > A). Orphanet J Rare Dis 2014;9:96